Ab Initio Potential Energy Surfaces for the Ground ($\tilde{X}^1A'$) and Excited ($\tilde{A}^1A''$) Electronic States of HGeBr and the Absorption and Emission Spectra of HGeBr/DGeBr†

Sen Lin and Daiqian Xie*

Institute of Theoretical and Computational Chemistry, Key Laboratory of Mesoscopic Chemistry, School of Chemistry and Chemical Engineering, Nanjing University, Nanjing 210093, China

Hua Guo*

Department of Chemistry and Chemical Biology, University of New Mexico, Albuquerque, New Mexico 87131

Received: December 12, 2008; Revised Manuscript Received: January 23, 2009

We report global potential energy surfaces for both the ground ($\tilde{X}^1A'$) and the excited ($\tilde{A}^1A''$) electronic states of HGeBr as well as the transition dipole moment surface between them using an internally contracted multireference configuration interaction method with the Davidson correction and an augmented correlation-consistent polarized valence quadruple-ζ basis set. Vibrational energy levels of HGeBr and DGeBr are calculated on both the ground and the excited electronic states and found in good agreement with the available experimental band origins. In addition, the $\tilde{A}^1A''-\tilde{X}^1A'$ absorption and emission spectra of the two isotopomers were obtained, and an excellent agreement with the available experimental spectra was found.

I. Introduction

The formation of silicon and germanium thin films by chemical vapor deposition (CVD) is known to involve many transient gas-phase species.[1−3] Because these intermediates are typically short-lived and highly reactive, they are difficult to monitor. To gain a better understanding of the CVD mechanism and kinetics, there is a keen interest in developing a definitive spectroscopic signature for these species. Although there are ample spectroscopic data for silylenes and its halogenated analogs (SiH_2 and SiHX (X = F, Cl, Br, I)),[4−9] the spectroscopic knowledge of the corresponding germylenes is until recently quite limited.

In this work, we focus on the monobromogermylene (HGeBr) system, which was first observed by Isabel and Guillory in 1972.[10] Using vacuum UV to photolyze H_3GeBr in an argon matrix, these authors observed the ground-state vibrational fundamentals of HGeBr and DGeBr by infrared absorption spectroscopy and determined a simple valence force field. In 1991, laser-induced fluorescence spectra of HGeBr for the $\tilde{A}^1A''-\tilde{X}^1A'$ transition were obtained by reacting germane (GeH_4) with bromine atoms.[11] Molecular constants of HGeBr were obtained by a least-squares analysis of the observed K subbands. The first spectra of jet-cooled HGeBr using a pulsed discharge technique were obtained about 10 years ago by Harper and Clouthier, and the vibrational and rotational structures of HGeBr were successfully resolved.[12] More recently, 37 ground-state vibrational levels of HGeBr and 45 of DGeBr were observed by Clouthier and co-workers from single vibronic level dispersed fluorescence spectra of jet-cooled HGeBr and DGeBr by laser excitation of selected bands.[13]

Only a few theoretical studies have been reported for monohalogermylenes.[14−19] Among these studies, a multireference single and double configuration interaction (MRSDCI) study of the three lowest-lying electronic states of HGeX (X = Cl, Br, I) by Benavides-Garcia and Balasubramanian in 1992 reported geometries, term values, and dipole moments.[15] Very recently, potential energy surfaces (PESs) of both the ground ($\tilde{X}^1A'$) and the excited ($\tilde{A}^1A''$) electronic states of HGeCl were reported by Lin et al.[19] Dynamic calculations on these PESs yielded both vibrational and electronic spectra of the molecule, and they were found to be in excellent agreement with available experimental data.[19]

TABLE 1: Geometrical Parameters for the Ground and Excited States of HGeBr

electronic state	method	R_e(HGe) (Å)	R_e(GeBr) (Å)	θ_e(HGeBr) (deg)
$\tilde{X}^1A'$	MRCI[a]	1.600	2.351	93.4
	MRSDCI[b]	1.572	2.388	93.9
	B3LYP[c]	1.600	2.370	93.5
	CCSD(T)[c]	1.582	2.337	93.6
	expt.[d]	1.630	2.330	103.0
	expt.[e]	1.598	2.329	93.9
$\tilde{A}^1A''$	MRCI[a]	1.593	2.326	115.2
	MRSDCI[b]	1.594	2.368	116.3
	expt.[d]	1.560	2.300	112.0
	expt.[e]	1.615	2.308	116.3

[a] This work. [b] Reference 15. [c] Reference 13. [d] Reference 11. [e] Reference 12.

In the present work, we extend our previous work on the HGeCl system[19] by reporting accurate ab initio PESs for both the ground ($\tilde{X}^1A'$) and the excited ($\tilde{A}^1A''$) electronic states of HGeBr using an internally contracted multireference configuration interaction method with the Davidson correction (MRCI+Q) and an augmented correlation-consistent polarized valence quadruple-ζ (AVQZ) basis set. Because of the heavier Br, the ab initio calculations are much more difficult. The vibrational energy levels on both electronic states as well as the absorption and emission spectra were calculated and compared to the available experimental data. The excellent agreement demonstrates that the PESs are very accurate. This Article is organized as follows. Section II outlines the details of the ab initio calculations and the variational calculations of the vibrational energy levels. Section III discusses the main

† Part of the "Robert Benny Gerber Festschrift".

* Corresponding authors. E-mail: dqxie@nju.edu.cn (D.X.); hguo@unm.edu (H.G.).

10.1021/jp810990j CCC: $40.75
Published on Web 03/16/2009

TABLE 2: Calculated Vibrational Energy Levels (in cm^{-1}) and Comparison with Experimental Results for HGeBr ($\tilde{X}^1A'$)

(n_1,n_2,n_3)	this work	expt.[a]	(n_1,n_2,n_3)	this work	expt.[a]	(n_1,n_2,n_3)	this work	expt.[a]	(n_1,n_2,n_3)	this work	expt.[a]
(0,0,0)	0.0		(0,2,13)	4967.33		(0,5,1)	3739.26	3709	(0,7,4)	5873.38	
(0,0,1)	287.65	291	(0,4,8)	4979.44		(0,1,11)	3760.18		(0,1,19)	5873.61	
(0,0,2)	573.83	579	(1,3,4)	5011.76		(0,3,6)	3765.08		(1,6,0)	5878.89	
(0,1,0)	698.84	694	(2,0,5)	5038.14		(1,2,2)	3772.91		(2,0,8)	5880.53	
(0,0,3)	858.70		(1,1,9)	5041.97		(1,0,7)	3820.75		(3,0,2)	5889.66	
(0,1,1)	984.88	983	(0,7,1)	5057.73		(1,3,0)	3885.95	3860	(2,3,1)	5895.68	
(0,0,4)	1142.15		(0,1,16)	5087.81		(0,0,14)	3888.00		(0,3,14)	5901.25	
(0,1,2)	1269.48	1270	(0,5,6)	5106.01		(2,0,1)	3894.82		(0,5,9)	5904.09	
(0,2,0)	1396.19	1384	(0,3,11)	5110.91		(0,2,9)	3896.33		(1,4,5)	5954.61	
(0,0,5)	1423.83		(1,4,2)	5123.48		(0,4,4)	3896.41		(3,1,0)	5966.18	
(0,1,3)	1552.72		(2,1,3)	5135.59		(1,1,5)	3940.78		(1,2,10)	5972.86	
(0,2,1)	1680.62	1671	(1,2,7)	5164.88		(0,5,2)	4016.06	3987	(0,8,2)	5981.04	
(0,0,6)	1703.57		(1,0,12)	5186.31		(0,1,12)	4029.02		(2,1,6)	5982.38	
(0,1,4)	1834.56		(0,0,19)	5201.38		(0,3,7)	4037.14		(1,0,15)	5984.30	
(1,0,0)	1835.61	1835	(0,6,4)	5223.16		(1,2,3)	4055.59		(0,2,17)	6017.44	
(0,2,2)	1963.57	1956	(1,5,0)	5226.52		(1,0,8)	4096.73		(0,6,7)	6024.66	
(0,0,7)	1981.60		(2,2,1)	5230.80		(0,6,0)	4126.45	4101	(0,0,22)	6036.01	
(0,3,0)	2092.75	2069	(0,2,14)	5231.76		(0,0,15)	4153.09		(0,4,12)	6039.89	
(0,1,5)	2114.72		(0,4,9)	5246.43		(0,2,10)	4166.01		(1,5,3)	6060.39	
(1,0,1)	2124.07	2126	(1,3,5)	5289.08		(1,3,1)	4169.17		(2,2,4)	6081.88	
(0,2,3)	2245.28		(3,0,0)	5310.32		(0,4,5)	4170.27		(0,9,0)	6087.70	
(0,0,8)	2258.31		(1,1,10)	5312.08		(2,0,2)	4182.76		(1,3,8)	6105.58	
(0,3,1)	2375.30	2354	(2,0,6)	5320.44		(1,1,6)	4219.59		(1,1,13)	6113.20	
(0,1,6)	2393.00		(0,7,2)	5331.12		(2,1,0)	4276.10		(0,7,5)	6140.88	
(1,0,2)	2411.02		(0,1,17)	5348.70		(0,5,3)	4291.67		(0,1,20)	6143.87	
(1,1,0)	2520.54	2514	(0,5,7)	5373.21		(0,1,13)	4296.28		(1,6,1)	6156.51	
(0,2,4)	2525.49		(0,3,12)	5375.80		(0,3,8)	4307.62		(2,0,9)	6158.41	
(0,0,9)	2533.84		(1,4,3)	5402.38		(1,2,4)	4336.75		(0,3,15)	6161.94	
(0,3,2)	2656.44	2638	(2,1,4)	5419.26		(1,0,9)	4371.42		(0,5,10)	6167.86	
(0,1,7)	2669.46		(0,8,0)	5435.35	5429	(0,6,1)	4402.71		(3,0,3)	6177.26	
(1,0,3)	2696.74		(1,2,8)	5435.91		(0,0,16)	4416.14		(2,3,2)	6179.56	
(0,4,0)	2783.14	2751	(1,0,13)	5454.31		(0,2,11)	4434.42		(1,4,6)	6226.89	
(0,2,5)	2803.61		(0,0,20)	5470.05		(0,4,6)	4441.73		(1,2,11)	6239.17	
(1,1,1)	2807.44		(0,6,5)	5492.44		(1,3,2)	4451.47		(1,0,16)	6246.34	
(0,0,10)	2808.05		(0,2,15)	5494.82		(2,0,3)	4469.32		(0,8,3)	6251.83	
(0,3,3)	2936.29		(1,5,1)	5505.70		(1,1,7)	4495.96		(3,1,1)	6255.25	
(0,1,8)	2944.32		(0,4,10)	5512.21		(0,1,14)	4561.86		(2,1,7)	6261.66	
(1,0,4)	2981.07		(2,2,2)	5515.96		(1,4,0)	4562.12		(2,4,0)	6273.21	
(0,4,1)	3063.51	3034	(1,3,6)	5563.83		(2,1,1)	4563.95		(0,2,18)	6279.51	
(0,2,6)	3079.32		(1,1,11)	5580.67		(0,5,4)	4565.55		(0,6,8)	6288.81	
(0,0,11)	3080.83		(3,0,1)	5600.72		(0,3,9)	4576.76		(0,4,13)	6301.64	
(1,1,2)	3092.90		(2,0,7)	5601.19		(1,2,5)	4615.67		(0,0,23)	6334.84	
(1,2,0)	3203.77	3189	(0,7,3)	5603.25		(1,0,10)	4644.72		(1,5,4)	6335.49	
(0,3,4)	3214.64		(0,1,18)	5609.72		(0,0,17)	4677.50		(0,1,9)	6359.95	
(0,1,9)	3217.75		(2,3,0)	5612.02		(0,6,2)	4677.63		(2,2,5)	6362.54	
(1,0,5)	3263.35		(0,5,8)	5639.16		(0,2,12)	4701.53		(1,3,9)	6373.30	
(0,4,2)	3342.50	3315	(0,3,13)	5639.26		(0,4,7)	4711.29		(1,1,14)	6377.11	
(0,0,12)	3351.55		(1,4,4)	5679.62		(1,3,3)	4732.39		(0,7,6)	6406.12	
(0,2,7)	3353.35		(2,1,5)	5701.42		(2,0,4)	4754.47		(0,3,16)	6419.49	
(1,1,3)	3377.02		(1,2,9)	5705.28		(1,1,8)	4769.97		(0,1,21)	6425.47	
(0,5,0)	3461.08	3428	(0,8,1)	5708.89		(0,7,0)	4782.96	4768	(0,5,11)	6430.28	
(1,2,1)	3488.98	3477	(1,0,14)	5720.31		(0,1,15)	4825.68		(1,6,2)	6432.32	
(0,1,10)	3489.66		(0,0,21)	5747.49		(0,5,5)	4836.99		(2,0,10)	6434.80	
(0,3,5)	3491.04		(0,2,16)	5756.75		(1,4,1)	4843.23		(2,3,3)	6461.72	
(1,0,6)	3543.15		(0,6,6)	5759.38		(0,3,10)	4844.56		(3,0,4)	6463.69	
(2,0,0)	3605.47	3601	(0,4,11)	5776.72		(2,1,2)	4850.45		(1,4,7)	6496.53	
(0,4,3)	3620.25		(1,5,2)	5783.69		(1,2,6)	4891.64		(1,2,12)	6503.96	
(0,0,13)	3620.80		(2,2,3)	5799.72		(1,0,11)	4916.41		(1,0,17)	6507.02	
(0,2,8)	3625.46		(1,3,7)	5835.89		(0,0,18)	4938.40		(0,8,4)	6520.45	
(1,1,4)	3659.77		(1,1,12)	5847.71		(2,2,0)	4944.79		(1,7,0)	6522.41	6499

[a] Taken from ref 12.

features of the new PESs, vibrational states, and electronic spectra, respectively. A brief summary is given in section IV.

II. Computational Details

A. Potential Energy and Transition Dipole Moment Surfaces. The electronic energies of the ground and excited electronic states of HGeBr were calculated using the MOLPRO suite of ab initio programs[20] using the multireference configuration interaction method with Davidson correction (MRCI+Q).[21−23] Dunning's AVQZ basis set[24] was used, which generated a total of 232 cGTOs.

The two PESs were constructed independently. For the ground ($\tilde{X}^1A'$) electronic state, all of the reference states were taken from the natural orbitals obtained from a state-averaged

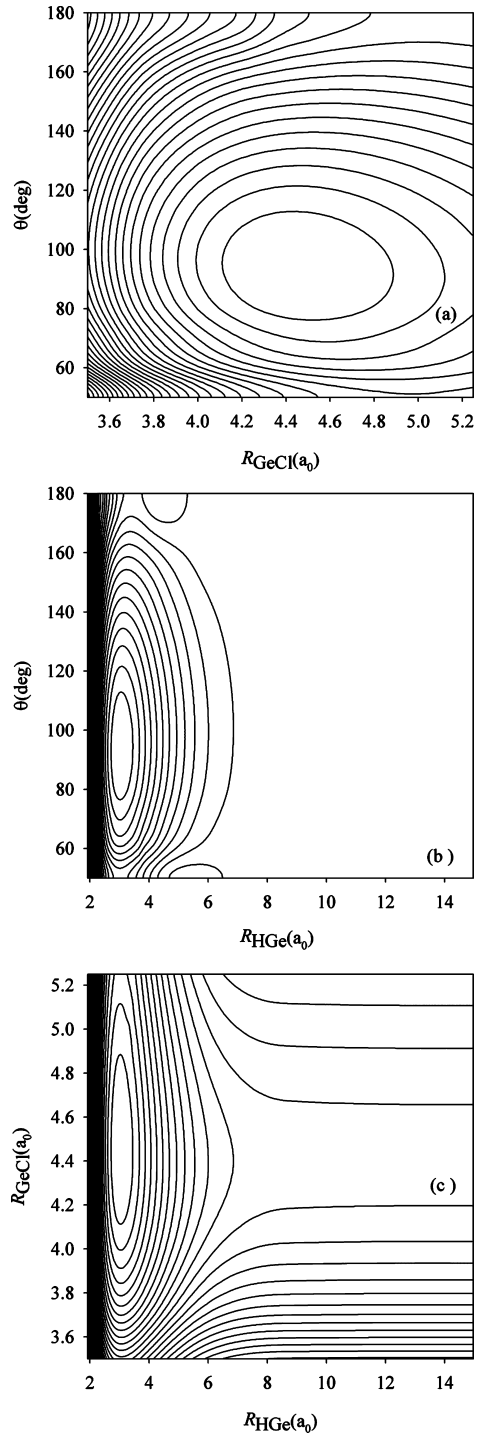

Figure 1. Potential energy surface of HGeBr ($\tilde{X}^1A'$) in internal coordinates. (a) Contour plot at $R_{HGe} = 3.024a_0$. (b) Contour plot at $R_{GeBr} = 4.445a_0$. (c) Contour plot at $\theta = 93.4°$. Contours are spaced by 0.25 eV with the zero defined at the HGeBr ($\tilde{X}^1A'$) minimum.

complete active space self-consistent field (CASSCF) calculation[25,26] for equally weighted $\mathbf{1}^1A'$, $\mathbf{1}^3A''$, and $\mathbf{1}^1A''$ states.[15] The CASSCF wave function includes 12 active electrons and 9 active orbitals (one for H, four for Ge, and four for Br). The remnant 28 core orbitals were fully optimized, while constrained to be doubly occupied. In the following MRCI calculations, the reference functions were taken as the same as the CASSCF active space. The total number of contracted configurations is about 1.23×10^8, significantly larger than that used for the HGeCl calculations.[19] All calculations were carried out in C_s symmetry. A nonuniform direct product grid in the internal coordinates (R_{HGe}, R_{GeBr}, θ) was selected for the calculations of the PES. Twenty-three points from 1.92 to $15.0a_0$ for R_{HGe} and 15 points from 3.50 to $5.30a_0$ for R_{GeBr} were chosen. In the angle direction, 15 points were used ranging from 50° to 180°. This gives a total of 5175 geometry points. We have also calculated the only nonzero ($\tilde{A}^1A''-\tilde{X}^1A'$) transition dipole moment, which is perpendicular to the molecular plane, using the same method. To overcome occasional convergence difficulties with the MRCI calculations, we have used the converged natural orbitals of a nearby geometry as the initial guess to resolve the convergence problem.

For the excited electronic state ($\tilde{A}^1A''$) of HGeBr, the CASSCF step contains $\mathbf{1}^1A''$ and $\mathbf{2}^1A''$ states for state-averaged calculations. To further consider the core-valence correlation effect,[27] we used a larger number of the active orbitals (14) with 22 electrons. The remnant 23 core orbitals were fully optimized, while constrained to be doubly occupied. In the subsequent MRCI calculations, the reference functions were taken as the same as the CASSCF active space. The total number of contracted configurations is about 1.69×10^9, much larger than that of the ground state. However, we have calculated fewer points for this PES because only the lowest-lying vibrational levels are of interest. In particular, 16 points from 2.25 to $4.75a_0$ for R_{HGe} and 10 points from 3.85 to $4.95a_0$ for R_{GeBr} were chosen. In the angular direction, 11 points were used ranging from 60° to 180°. A total of 1766 points were generated.

Finally, both PESs and the transition dipole function at any arbitrary point were obtained using a three-dimensional cubic spline interpolation. The FORTRAN code for the PESs and the transition dipole is available upon request.

B. Vibrational Energy Levels. The triatomic vibrational Hamiltonian with the total angular momentum $J = 0$ in the Radau coordinates (R_1, R_2, γ) is given below:

$$\hat{H} = -\frac{\hbar^2}{2m_1}\frac{\partial^2}{\partial R_1^2} - \frac{\hbar^2}{2m_2}\frac{\partial^2}{\partial R_2^2} - \frac{\hbar^2}{2}\left(\frac{1}{m_1R_1^2} + \frac{1}{m_2R_2^2}\right)\left(\frac{\partial^2}{\partial\gamma^2} + \cot\gamma\frac{\partial}{\partial\gamma}\right) + V(R_1, R_2, \gamma) \quad (1)$$

where m_1 and m_2 are the atomic mass of H and Br, respectively. The Radau coordinates (R_1, R_2, γ) can be readily transformed to the internal bond length−bond angle coordinates (R_{HGe}, R_{GeBr}, θ), and vice versa.[28]

The Hamiltonian in eq 1 was discretized in a direct product discrete variable representation (DVR) grid.[29] The lowest-lying eigenvalues are then extracted using the recursive Lanczos algorithm.[30] When eigenfunctions are required, they are generated by additional Lanczos recursions. Extensive convergence tests were carried out to ascertain the accuracy of the results with respect to the number of recursion steps and grid size.

For the ground electronic state, R_1 and R_2 were represented by potential optimized DVRs (PODVRs)[31,32] with 80 and 50 grid points. These PODVR points were obtained by diagonalizing the coordinate matrices in the one-dimensional eigenbases of the reduced Hamiltonians in the two coordinates, respectively. Ninety Gauss−Legendre[33] grid points in the interval [50°, 180°] were used for γ. The converged vibrational energy levels below 6500 cm^{-1} were generated by performing about 10 000 Lanczos recursion steps with a cutoff of 4.0 eV for the potential energy.

For the excited electronic state of HGeBr, different parameters were used for calculating the vibrational states because only the low-lying vibrational levels are of interest here. The PODVR

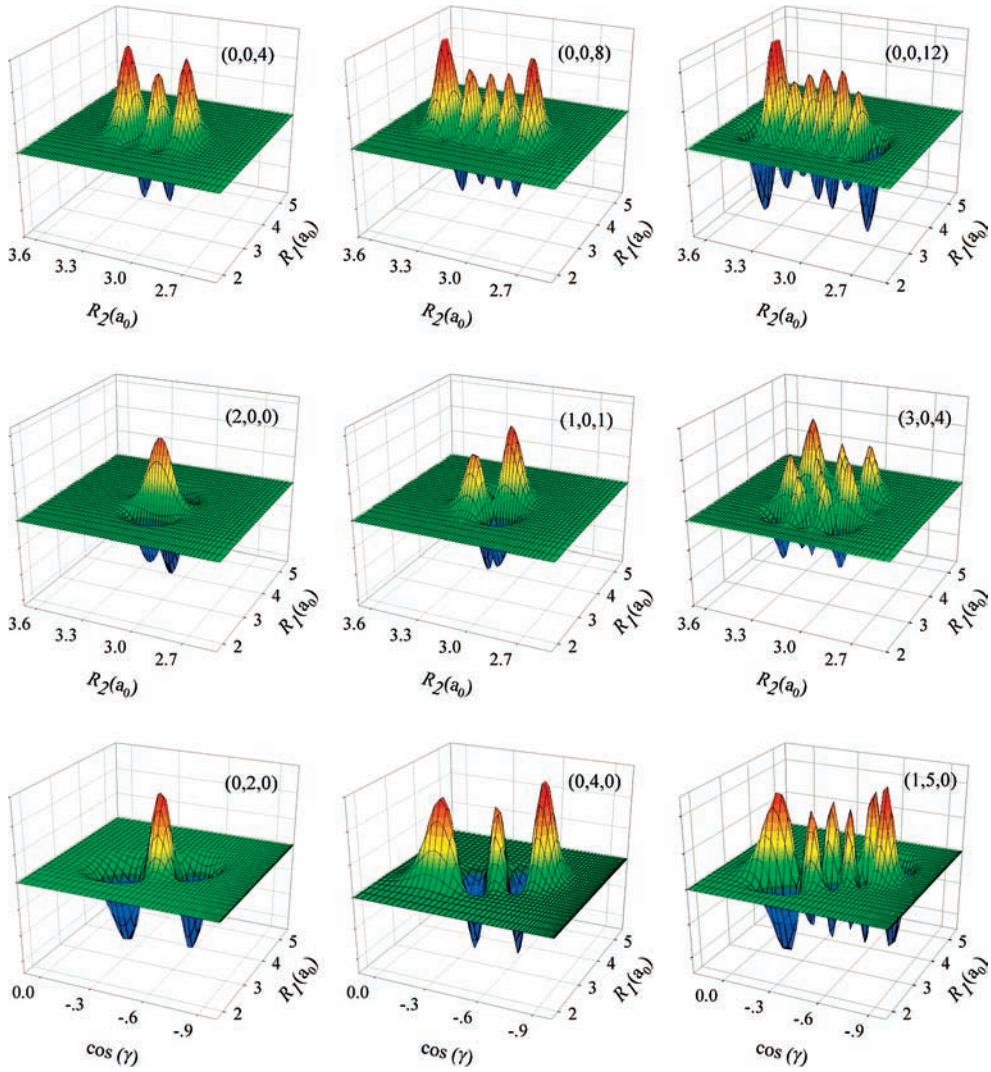

Figure 2. Contour plots of nine vibrational eigenfunctions of HGeBr ($\tilde{X}^1A'$) in Radau coordinates. The three vibrational quantum numbers (n_1, n_2, n_3) represent the H−Ge stretching, bending, and Ge−Br stretching modes, respectively.

grids for R_1 and R_2 consist of 60 and 40 points, respectively. Eighty Gauss−Legendre grid points in the interval [60°, 180°] were used for γ. The converged vibrational energy levels below 2000 cm^{-1} were generated by performing about 2000 Lanczos recursion steps with a cutoff of 2.5 eV for the potential energy.

C. Absorption and Emission Spectra. The absorption and emission spectra were calculated as

$$\sum(\omega) \propto |\langle \Phi_n|\mu|\Psi_{n'}\rangle|^2 \quad (2)$$

where μ is the transition dipole, and Φ_n and $\Psi_{n'}$ are the vibrational eigenfunctions of the ground and excited electronic state Hamiltonians, respectively. The transition amplitude $\langle \Phi_n|\mu|\Psi_{n'}\rangle$ can, of course, be calculated directly from the vibrational eigenfunctions on the two electronic states, but we have, in this work, used the efficient single Lanczos propagation (SLP) method.[34,35] This method is particularly efficient for calculating emission from multiple excited-state levels because it requires no explicit construction and storage of the vibrational eigenfunctions, and it has been proved successful in a number of systems.[36]

For the calculation of electronic spectra, the vibrational Hamiltonians for both the ground and the excited electronic states need to be represented by the same DVR grid. For this reason, 80 sine-DVR points were employed to cover the R_1 range of [1.95, 6.00]a_0 and 60 sine-DVR points for the R_2 range of [2.65, 3.45]a_0. For γ, a 90-point Gauss−Legendre DVR grid in the range of [60°, 180°] was used.

III. Results and Discussion

A. Ground ($\tilde{X}^1A'$) State Potential and Vibrational Energy Levels. The ground electronic state PES of HGeBr contains a global minimum located at $R_{HGe} = 3.024a_0$, $R_{GeBr} = 4.445a_0$, and $\theta = 93.4°$. No other minimum was found in the region of ab initio calculations. The equilibrium geometry of HGeBr is very similar to that of HGeCl,[19] except for a longer Ge−Br bond. Our results are compared in Table 1 with previous experimental data and theoretical results. It is clear that our equilibrium geometry is in good agreement with these experimental and theoretical values.[11−13,15] The calculated dissociation energy for the H−Ge bond, D_e(HGeBr → GeBr + H), is about 70.40 kcal/mol, which is similar to the calculated value of HGeCl.[19] The corresponding value for the breaking of the Ge−Br bond is not available from our calculations because of insufficient grid points in the R_{GeBr} coordinate.

Figure 1 shows the contour plots of the ground electronic state PES of HGeBr in internal coordinates (R_{HGe}, R_{GeBr}, θ). Panel (a) displays its dependence on R_{GeBr} and the interbond angle θ with R_{HGe} fixed at its equilibrium value of $3.024a_0$. In

TABLE 3: Comparison of Calculated Vibrational Energy Levels (in cm^{-1}) with Experimental Results for DGeBr ($\tilde{X}^1A'$)

(n_1,n_2,n_3)	this work	expt.[a]	(n_1,n_2,n_3)	this work	expt.[a]
(0,0,0)	0.0		(0,5,2)	3062.18	3036
(0,0,1)	287.40	290	(1,3,1)	3088.92	3078
(0,1,0)	501.41	498	(0,6,1)	3273.27	3240
(0,1,1)	787.62	787	(1,4,0)	3299.29	3275
(0,2,0)	1001.53	994	(0,7,0)	3479.77	3445
(0,2,1)	1286.56	1283	(0,6,2)	3550.97	3518
(1,0,0)	1322.48	1322	(1,4,1)	3580.15	3560
(0,3,0)	1502.62	1489	(0,7,1)	3756.99	3724
(0,2,2)	1570.14	1566	(1,5,0)	3790.36	3758
(1,0,1)	1610.43	1614	(0,8,0)	3958.44	3929
(0,3,1)	1786.41	1775	(1,5,1)	4067.15	4040
(1,1,0)	1817.12	1813	(0,8,1)	4234.16	4205
(0,4,0)	2004.14	1982	(1,6,0)	4275.64	4239
(0,3,2)	2068.76	2060	(0,9,0)	4431.49	4410
(1,1,1)	2103.95	2104	(1,6,1)	4551.11	4521
(0,4,1)	2286.43	2266	(0,9,1)	4705.93	4686
(1,2,0)	2310.50	2303	(1,7,0)	4754.32	4718
(0,5,0)	2502.28	2471	(0,10,0)	4901.01	4889
(0,4,2)	2567.37	2549	(1,7,1)	5029.41	4996
(1,2,1)	2596.15	2592	(1,8,0)	5226.61	5194
(0,5,1)	2782.83	2754	(1,9,0)	5693.54	5670
(1,3,0)	2804.78	2790	(1,10,0)	6157.05	6142
(0,6,0)	2994.44	2959	(1,11,0)	6619.29	6610

[a] Taken from ref 12.

TABLE 4: Calculated Vibrational Energy Levels (in cm^{-1}) and Comparison with Experimental Results for HGeBr ($\tilde{A}^1A''$)

(n_1,n_2,n_3)	this work	expt.[a]	(n_1,n_2,n_3)	this work	expt.[a]
(0,0,0)	0.0		(0,0,5)	1391.86	
(0,0,1)	282.23	280.32	(1,0,0)	1438.19	1380.82
(0,1,0)	421.38	419.31	(0,3,1)	1466.95	
(0,0,2)	563.03		(0,4,0)	1508.85	
(0,1,1)	702.62	696.57	(0,1,4)	1534.98	
(0,2,0)	823.23	811.38	(0,5,0)	1568.68	
(0,0,3)	841.59		(0,2,3)	1657.26	
(0,1,2)	982.25		(0,0,6)	1664.75	
(0,2,1)	1103.20	1081.35	(0,6,0)	1709.46	
(0,0,4)	1117.71		(1,0,1)	1720.76	
(0,3,0)	1195.74	1146.84	(0,3,2)	1749.02	
(0,1,3)	1259.77		(0,4,1)	1793.66	
(0,2,2)	1381.31		(1,1,0)	1802.78	1726.99

[a] Taken from ref 13.

panel (b), the variation in R_{HGe} and θ coordinates is displayed with R_{GeBr} fixed at its equilibrium value of $4.445a_0$. The last panel (c) shows the variation in two bond lengths when the interbond angle is fixed at 93.4°.

The calculated vibrational levels for the ground electronic state ($\tilde{X}^1A'$) of HGeBr are listed in Table 2 up to 6500 cm^{-1}. They are compared in the same table with the available experimental band origins. The vibrational energy levels are assigned with three vibrational quantum numbers (n_1, n_2, n_3), representing the H−Ge stretching, bending, and Ge−Br stretching vibrations, respectively. The assignment of the vibrational levels was achieved by inspecting the nodal structures of the corresponding eigenfunctions in the Radau coordinates. Wave functions of nine representative vibrational levels are displayed in Figure 2, in which the nodal structures are clearly visible. The ease of the assignment suggests that the vibration of HGeBr is largely regular with little intramodal coupling, at least in this spectral region.

It is apparent from Table 2 that the calculated vibrational energy levels reproduce the available experimental band origins

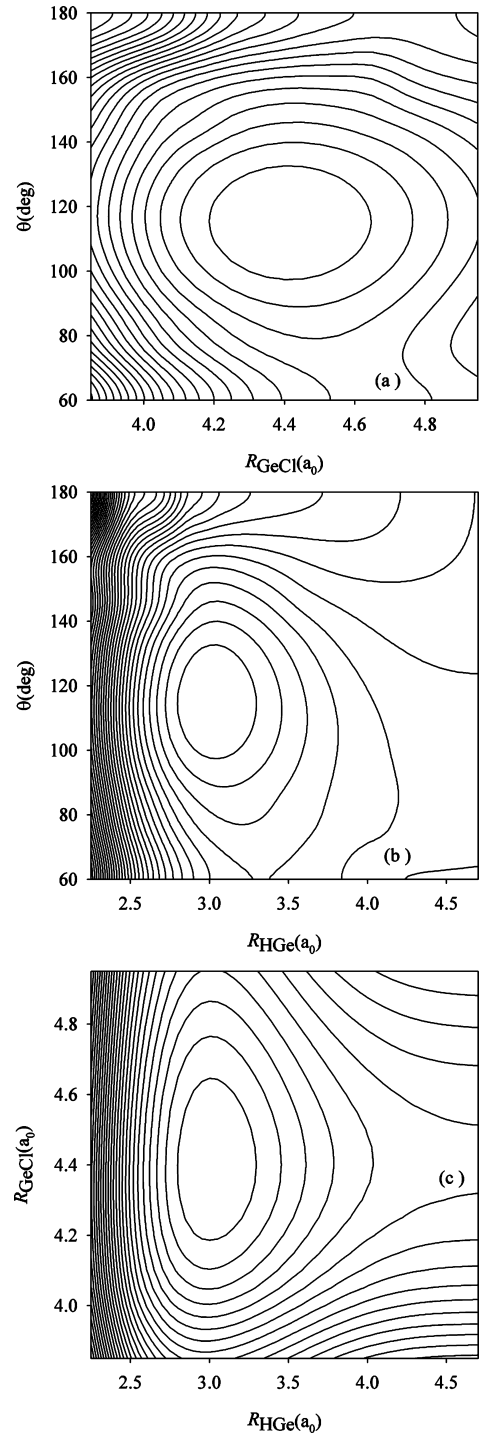

Figure 3. Potential energy surface of HGeBr ($\tilde{A}^1A''$) in internal coordinates. (a) Contour plot at $R_{HGe} = 3.011a_0$. (b) Contour plot at $R_{GeBr} = 4.397a_0$. (c) Contour plots at $\theta = 115.2°$. Contours are spaced by 0.085 eV with the zero defined at the HGeBr ($\tilde{A}^1A''$) minimum.

quite well. The fundamental frequency for the H−Ge stretching mode (1835.61 cm^{-1}) is in excellent agreement with that of Tackett et al. (1835 cm^{-1}).[13] On the other hand, the calculated fundamental frequencies of the Ge−Br stretching and bending modes (287.66 and 698.84 cm^{-1}) are, respectively, in good agreement with the latest experimental values (291 and 694 cm^{-1}).[13] The good theory−experiment agreement is held all of the way to the highest experimentally assigned level (1, 7, 0) near 6500 cm^{-1}.

The vibrational energy levels of DGeBr have also been obtained on the same ab initio PES. A selected list of vibrational

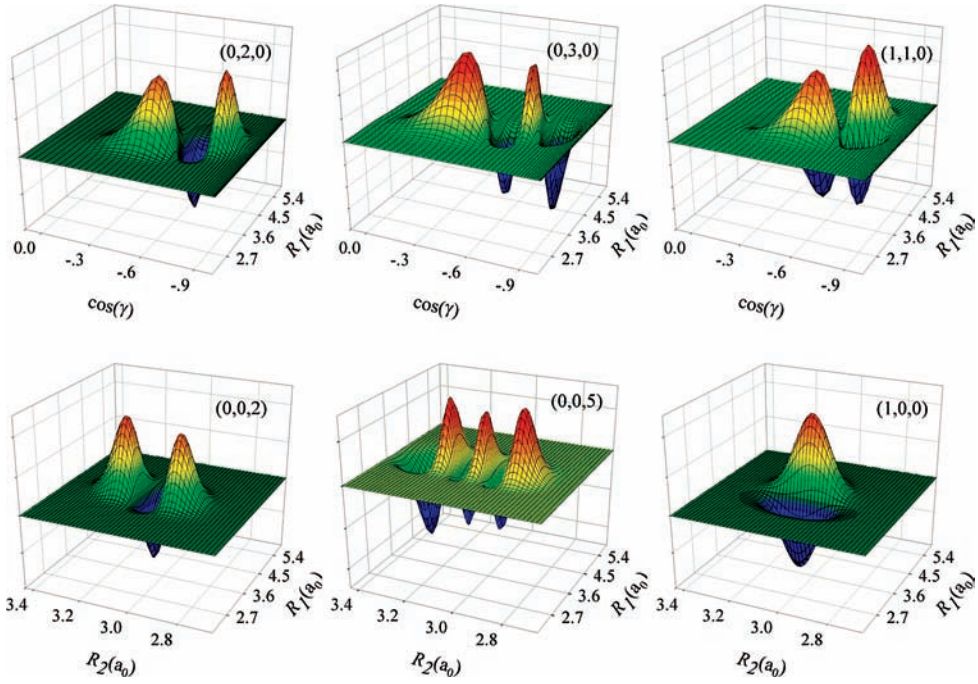

Figure 4. Contour plots of six vibrational eigenfunctions of HGeBr ($\tilde{A}^1A''$) in Radau coordinates. The three vibrational quantum numbers (n_1, n_2, n_3) represent the H−Ge stretching, bending, and Ge−Br stretching modes, respectively.

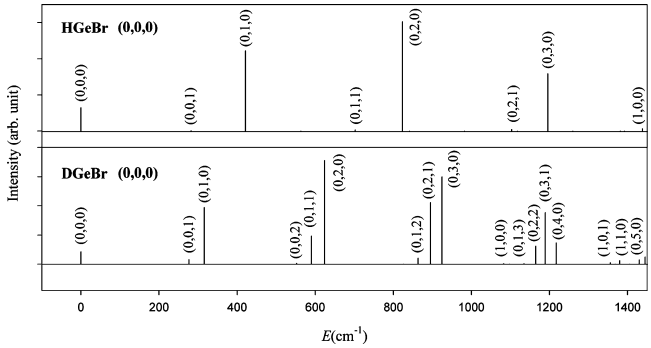

Figure 5. Calculated stick absorption spectra for the $\tilde{A}^1A''$←$\tilde{X}^1A'$ transition from the lowest vibrational level $\tilde{X}$(0, 0, 0) of HGeBr and DGeBr, respectively.

TABLE 5: Calculated Vibrational Energy Levels (in cm^{-1}) and Comparison with Experimental Results for DGeBr ($\tilde{A}^1A''$)

(n_1,n_2,n_3)	this work	expt.[a]	(n_1,n_2,n_3)	this work	expt.[a]
(0,0,0)	0.0		(0,1,3)	1134.88	
(0,0,1)	276.68	278.49	(0,2,2)	1164.92	
(0,1,0)	315.80	312.14	(0,3,1)	1189.46	
(0,0,2)	552.22		(0,4,0)	1217.45	1157.04
(0,1,1)	590.05	588.80	(1,0,1)	1355.78	1321.32
(0,2,0)	624.12	613.35	(1,1,0)	1379.61	1334.99
(0,1,2)	863.22		(0,5,0)	1429.94	
(0,2,1)	895.40	887.61	(1,3,0)	1892.16	1836.53
(0,3,0)	924.94	899.57	(2,0,0)	2027.96	1947.56
(1,0,0)	1082.94	1047.60	(2,1,0)	2278.20	2184.71

[a] Taken from ref 13.

levels is compared in Table 3 with available experimental band origins. Again, the calculated results are in excellent agreement with experiment. The fundamental vibrational frequency calculated for the D−Ge stretching mode of 1322.48 cm^{-1} reproduces the recent experimental value of 1322 cm^{-1} by Tackett et al.[13] The calculated values for the other two fundamental frequencies of 287.40 and 501.41 cm^{-1} are very close to the experimental values of 290 and 498 cm^{-1}, respectively. One can see from Tables 2 and 3 that all of the calculated vibrational energy levels for HGeBr/DGeBr are within 35 cm^{-1} of the observed values, demonstrating the high accuracy of the ab initio PES.

B. Excited ($\tilde{A}^1A''$) State Potential and Vibrational Energy Levels. Figure 3 displays the contour plots of the excited electronic state ($\tilde{A}^1A''$) PES for HGeBr in internal coordinates (R_{HGe}, R_{GeBr}, θ). The equilibrium geometry was found at $R_{HGe} = 3.011a_0$, $R_{GeBr} = 4.397a_0$, and $\theta = 115.2°$. In comparison with the ground state, neither the H−Ge nor the Ge−Br bond length is significantly different, but the bending angle is extended by approximately 20°. As discussed below, this geometric difference will manifest in both the absorption and the emission spectra. The MRCI equilibrium geometry compares well with previous experimental and theoretical values in Table 1.[11,12,15]

The calculated vibrational levels for the excited ($\tilde{A}^1A''$) electronic states of HGeBr and DGeBr are presented in Tables 4 and 5, respectively, together with the available experimental results. The energies given in the tables are relative to the ground (0, 0, 0) vibrational level on this PES. No absolute excitation energy is reported here because different theoretical treatments were used for the two electronic states. Figure 4 plots six representative wave functions of HGeBr on the excited electronic states, and their nodal structures are clearly shown. The calculated fundamental frequencies of the H−Ge stretching, Ge−Br stretching, and bending modes (1438.19, 282.23, and 421.38 cm^{-1}) are in reasonably good agreement with the experimental values (1380.82, 280.32, and 419.31 cm^{-1}).[12] The other vibrational levels calculated are also consistent with the available experimental band origins, but the errors are larger than those observed in the ground electronic state, as expected. A particularly larger difference is found between the calculated and observed H−Ge/D−Ge stretching frequencies, which is also seen in our earlier work on HGeCl.[19] Therefore, the PES of the $\tilde{A}^1A''$ state may require an even higher level of theory in terms of both the correlation method and the basis set used. In addition,

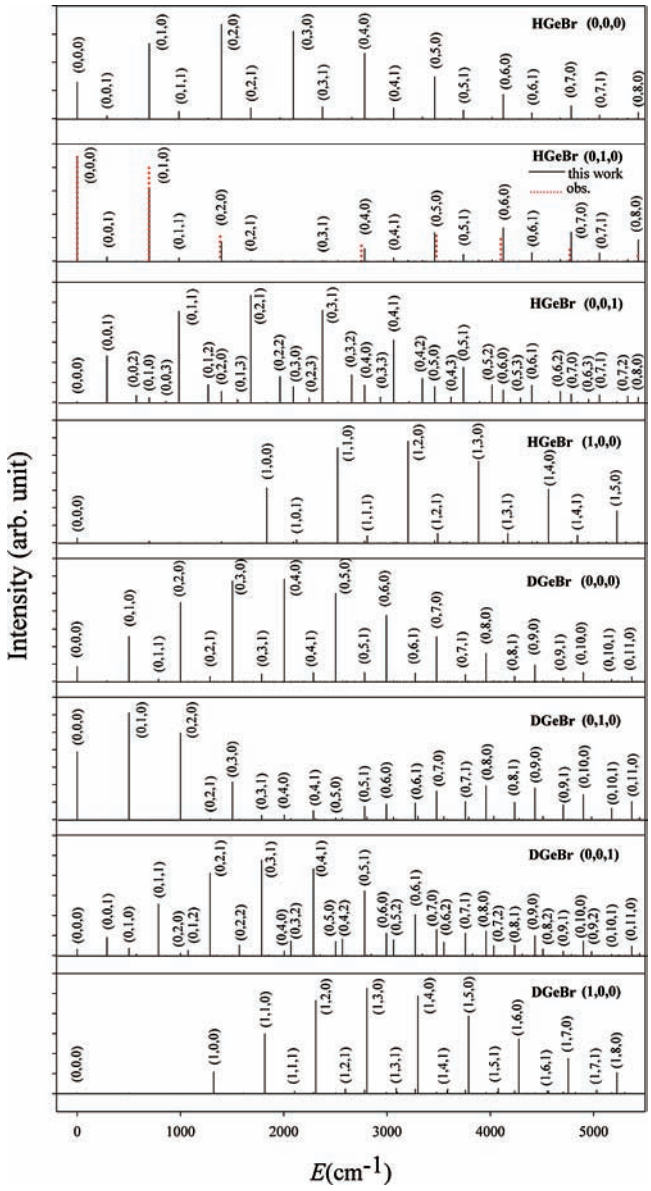

Figure 6. Calculated stick emission spectra for the $\tilde{A}^1A''\rightarrow\tilde{X}^1A'$ transition from several vibrational levels of HGeBr and DGeBr. The experimental spectra are taken from ref 13.

more core-valance correlation might have to be included to produce better vibrational frequencies.[27]

C. Absorption Spectra. The $\tilde{A}^1A''\leftarrow\tilde{X}^1A'$ electronic excitation involves a transition from a nonbonding nσ orbital to a vacant 4p orbital located on the germanium atom.[12] The only nonzero component of the transition dipole is perpendicular to the molecular plane, and it varies smoothly with the three coordinates in the Franck−Condon region (not shown here). Figure 5 displays the calculated $\tilde{A}^1A''\leftarrow\tilde{X}^1A'$ absorption spectra from the lowest vibrational state $\tilde{X}(0, 0, 0)$ of both HGeBr and DGeBr. The calculated spectra are found to contain a relatively small number of vibronic bands, and the intense lines in these spectra are labeled by (n_1, n_2, n_3) of the excited $\tilde{A}$ state. The spectral positions of the vibronic bands of HGeBr and DGeBr are consistent with the experimental spectra obtained with the laser-induced fluorescence technique.[12] Given the 20° change in the bending equilibrium angle, it can be expected that the absorption is dominated by excitation in the bending mode. Indeed, the absorption spectra for both HGeBr and DGeBr are dominated by the (0, n_2, 0) progression, although the latter is more congested due to the smaller frequencies. For HGeBr, our calculations identified several weaker bands such as (0, 0, 1), (0, 1, 1), (0, 2, 1), and (1, 0, 0). For its deuterated isotopomers DGeBr, more weak bands, (0, 0, 1), (0, 0, 2), (0, 1, 1), (0, 1, 2), (0, 2, 1), (1, 0, 0), (0, 1, 3), (0, 2, 2), (0, 3, 1), (1, 0, 1), and (1, 1, 0), were found.

D. Emission Spectra. The calculated $\tilde{A}^1A''\rightarrow\tilde{X}^1A'$ emission spectra from several low-lying states of HGeBr and DGeBr are shown in Figure 6. In the same figure, the positions and intensities of special lines derived from experimental data are also shown in dotted lines. The spectra are concentrated in the spectral region within 5500 cm^{-1} above the band origin, and it is clear that the experimental emission spectra of Tackett et al.[13] are well reproduced by the calculated spectra from the vibrational state of $\tilde{A}(0, 1, 0)$. As shown in this figure, the emission spectra from $\tilde{A}(0, 1, 0)$ are dominated by the (0, n_2, 0) progression and, to a lesser extent, the (0, n_2, 1) progression, which was not identified by experiment. The double maximum feature of the progression is apparently due to the node in the $\tilde{A}(0, 1, 0)$ wave function. The large bending excitations can again be attributed to the approximately 20° increase in the bond angle upon electronic excitation. The slight difference in the Ge−Br bond length between the two electronic states is responsible for the weaker (0, n_2, 1) progression. On the other hand, the virtually identical H−Ge bond length in the two electronic states results in no excitation in the H−Ge vibration. The excellent agreement between theory and experiment again suggests that both the ground and the excited-state PESs are quite reliable.

In addition, the emission spectra from the vibrational states of $\tilde{A}(0, 0, 0)$, $\tilde{A}(0, 0, 1)$, and $\tilde{A}(1, 0, 0)$, which were not identified in the experimental work of Tackett et al.,[13] were also calculated and plotted in the same figure. The calculated emission spectrum from the vibrational state of $\tilde{A}(0, 0, 0)$ differs from that of $\tilde{A}(0, 1, 0)$ in that there is not a dip near (0, 3, 0) because of the nodeless wave function. On the other hand, the emission spectrum from the vibrational state $\tilde{A}(0, 0, 1)$ of HGeBr is dominated by several bending progressions, with 0, 1, 2, and 3 quanta in the Ge−Br mode, respectively. Among them, the (0, n_2, 1) progression is the most intense, consistent with the vertical nature of the excitation. The emission spectrum from the $\tilde{A}(1, 0, 0)$ state of HGeBr is dominated by the (1, n_2, 0) progression, augmented by several weaker ones.

The essential features of the spectra are similar for the two isotopomers, but the DGeBr spectra are generally more congested than that of HGeBr due to the larger mass of deuterium. These emission spectra demonstrate that the spectral pattern is quite sensitive to the vibrational state from which emission originates. These observations are very similar to those made in our previous work on HGeCl.[19]

IV. Conclusions

A better understanding of vibrational and electronic spectra of transient molecules requires accurate potential energy surfaces of both the ground and the excited states. In this Article, we extend our recent work on halogenated germylenes by reporting accurate ab initio PESs for both the ground ($\tilde{X}^1A'$) and the excited electronic state ($\tilde{A}^1A''$) of HGeBr, as well as the $\tilde{A}^1A''-\tilde{X}^1A'$ transition dipole function. The nonempirical three-dimensional potential energy surfaces and transition dipole function are constructed by spline interpolation of numerous ab initio points, which were obtained at the MRCI+Q/AVQZ level of theory. Low-lying vibrational levels of both HGeBr and DGeBr have been determined using the recursive Lanczos

method. The calculated results are in excellent agreement with the experimental data, demonstrating the good quality of the ground-state PES. In addition, absorption and emission spectra of HGeBr/DGeBr were calculated using an efficient single Lanczos propagation method, and the resulting spectra were found to reproduce experimental observations. Like in HGeCl, the approximately 20° difference in the HGeBr equilibrium bending angle in the two electronic states leads to significant bending excitations in both absorption and emission spectra. Our theoretical results reported here provided much needed insight into the vibrational dynamics of HGeBr in both its ground and excited-state potentials.

Acknowledgment. This work was supported by the National Natural Science Foundation of China (grant nos. 20725312, 10574068, and 20533060) and by the Ministry of Science and Technology (2007CB815201). H.G. acknowledges support by the Department of Energy (DE-FG02-05ER15694).

References and Notes

(1) Steinfeld, J. I. *Chem. Rev.* **1989**, *89*, 1291.
(2) Osmundsen, J. F.; Abele, C. C.; Eden, J. G. *J. Appl. Phys.* **1985**, *57*, 2921.
(3) Lill, M.; Schroder, B. *Appl. Phys. Lett.* **1999**, *74*, 1284.
(4) Harper, W. W.; Hostutler, D. A.; Clouthier, D. J. *J. Chem. Phys.* **1997**, *106*, 4367.
(5) Harper, W. W.; Clouthier, D. J. *J. Chem. Phys.* **1997**, *106*, 9461.
(6) Clouthier, D. J.; Harper, W. W.; Klusek, C. M.; Smith, T. C. *J. Chem. Phys.* **1998**, *109*, 7827.
(7) Hostutler, D. A.; Ndiege, N.; Clouthier, D. J.; Pauls, S. W. *J. Chem. Phys.* **2001**, *115*, 5485.
(8) Hostutler, D. A.; Clouthier, D. J.; Judge, R. H. *J. Chem. Phys.* **2001**, *114*, 10728.
(9) Tackett, B. S.; Clouthier, D. J. *J. Chem. Phys.* **2003**, *118*, 2612.
(10) Isabel, R. J.; Guillory, W. A. *J. Chem. Phys.* **1972**, *57*, 1116.
(11) Ito, H.; Hirota, E.; Kuchitsu, K. *Chem. Phys. Lett.* **1991**, *177*, 235.
(12) Harper, W. W.; Clouthier, D. J. *J. Chem. Phys.* **1998**, *108*, 416.
(13) Tackett, B. S.; Li, Y.; Clouthier, D. J.; Pacheco, K. L.; Schick, G. A.; Judge, R. H. *J. Chem. Phys.* **2006**, *125*, 114301.
(14) Kerins, M. C.; Fitzpatrick, N. J.; Nguyen, M. T. *J. Mol. Struct. (THEOCHEM)* **1988**, *180*, 297.
(15) Benavides-Garcia, M.; Balasubramanian, K. *J. Chem. Phys.* **1992**, *97*, 7537.
(16) Olah, J.; Proft, F. D.; Veszpremi, T.; Geerlings, P. *J. Phys. Chem. A* **2004**, *108*, 490.
(17) Olah, J.; Proft, F. D.; Veszpremi, T.; Geerlings, P. *J. Phys. Chem. A* **2005**, *109*, 1608.
(18) Su, M.-D.; Chu, S.-Y. *J. Am. Chem. Soc.* **1999**, *121*, 4229.
(19) Lin, S.; Xie, D.; Guo, H. *J. Chem. Phys.* **2008**, *129*, 154313.
(20) Werner, H. J.; Knowles, P. J.; Amos, R. D. MOLPRO, a package of ab initio programs.
(21) Langhoff, S. R.; Davidson, E. R. *Int. J. Quantum Chem.* **1974**, *8*, 61.
(22) Werner, H.-J.; Knowles, P. J. *J. Chem. Phys.* **1988**, *89*, 5803.
(23) Knowles, P. J.; Werner, H.-J. *Chem. Phys. Lett.* **1988**, *145*, 514.
(24) Dunning, T. H., Jr. *J. Chem. Phys.* **1989**, *90*, 1007.
(25) Werner, H.-J.; Knowles, P. J. *J. Chem. Phys.* **1985**, *82*, 5053.
(26) Knowles, P. J.; Werner, H.-J. *Chem. Phys. Lett.* **1985**, *115*, 259.
(27) Mok, D. K. W.; Lee, E. P. F.; Chau, F.-T.; Dyke, J. M. *J. Chem. Phys.* **2004**, *120*, 1292.
(28) Johnson, B. R.; Reinhardt, W. P. *J. Chem. Phys.* **1986**, *85*, 4538.
(29) Light, J. C.; Hamilton, I. P.; Lill, J. V. *J. Chem. Phys.* **1985**, *82*, 1400.
(30) Lanczos, C. *J. Res. Natl. Bur. Stand.* **1950**, *45*, 255.
(31) Echave, J.; Clary, D. C. *Chem. Phys. Lett.* **1992**, *190*, 225.
(32) Wei, H.; Carrington, T. *J. Chem. Phys.* **1992**, *97*, 3029.
(33) Lill, J. V.; Parker, G. A.; Light, J. C. *Chem. Phys. Lett.* **1982**, *89*, 483.
(34) Chen, R.; Guo, H. *J. Chem. Phys.* **2001**, *114*, 1467.
(35) Chen, R.; Guo, H. *J. Chem. Phys.* **1999**, *111*, 9944.
(36) Guo, H.; Chen, R.; Xie, D. *J. Theor. Comput. Chem.* **2002**, *1*, 173.

JP810990J